Follow us @BoneJointRes

Freely available online OPEN ACCESS

BJR

CARTILAGE

Effect of treadmill training on fibrocartilage complex repair in tendon-bone insertion healing in the postinflammatory stage

J. Tan,
X. Liu,
M. Zhou,
F. Wang,
L. Ma,
H. Tang,
G. He,
X. Kang,
X. Bian,
K. Tang

From First Affiliated Hospital of Army Medical University, Chongqing, China

Aims

Mechanical stimulation is a key factor in the development and healing of tendon-bone insertion. Treadmill training is an important rehabilitation treatment. This study aims to investigate the benefits of treadmill training initiated on postoperative day 7 for tendon-bone insertion healing.

Methods

A tendon-bone insertion injury healing model was established in 92 C57BL/6 male mice. All mice were divided into control and training groups by random digital table method. The control group mice had full free activity in the cage, and the training group mice started the treadmill training on postoperative day 7. The quality of tendon-bone insertion healing was evaluated by histology, immunohistochemistry, reverse transcription quantitative polymerase chain reaction, Western blotting, micro-CT, micro-MRI, open field tests, and CatWalk gait and biomechanical assessments.

Results

Our results showed a significantly higher tendon-bone insertion histomorphological score in the training group, and the messenger RNA and protein expression levels of type II collagen (COL2A1), SOX9, and type X collagen (COL10A1) were significantly elevated. Additionally, tendon-bone insertion resulted in less scar hyperplasia after treadmill training, the bone mineral density (BMD) and bone volume/tissue volume (BV/TV) were significantly improved, and the force required to induce failure became stronger in the training group. Functionally, the motor ability, limb stride length, and stride frequency of mice with tendon-bone insertion injuries were significantly improved in the training group compared with the control group.

Conclusion

Treadmill training initiated on postoperative day 7 is beneficial to tendon-bone insertion healing, promoting biomechanical strength and motor function. Our findings are expected to guide clinical rehabilitation training programmes.

Cite this article: *Bone Joint Res* 2023;12(5):339–351.

Keywords: Tendon-bone insertion healing, Fibrocartilage complex, Treadmill training, Postinflammatory stage

Article focus

- To determine the effects of treadmill training initiated on postoperative day 7 on fibrocartilage complex repairing in tendon-bone insertion injury model, and on tendon-bone insertion injury repair in terms of motor function.

Key messages

- Treadmill training initiated on postoperative day 7 can promote structural reconstruction of the fibrocartilage complex. Treadmill training initiated on postoperative day 7 not only promoted chondrogenesis, but also enhanced the new bone

Correspondence should be sent to Xuting Bian; email: anthonybean@163.com

doi: 10.1302/2046-3758.125.BJR-2022-0340.R2

Bone Joint Res 2023;12(5):339–351.

formation. Tendon-bone insertion injury model mice showed significant improvement in motor function after treadmill training was initiated.

Strengths and limitations

- This study has demonstrated the reliability of this treadmill training programme in terms of cartilage and bone formation as well as motor function. Our findings are expected to guide clinical rehabilitation training programmes.
- This study has not elucidated the specific molecular mechanisms, and the mice model we constructed differs from the clinical human body.

Introduction

Tendon-bone insertion, which can also be described as enthesis, is a complex hierarchical tissue. The fibrocartilage complex is the crucial structure of tendon-bone insertion including tendon, non-calcified fibrocartilage, calcified fibrocartilage, and bone, which dissipates stress concentrations between tendon and bone. Tendon-bone insertion injury is commonly seen in sports medicine clinics and often occurs in the rotator cuff, Achilles tendon, and patellar tendon. Tendon-bone insertion injury damage levels are high and frequently disabling, and the incidence rate is increasing annually.[1,2] According to previous surveys,[3-5] the incidence of rotator cuff injury alone is 19.0% to 32.0%; in the USA, over 250,000 rotator cuff repair operations are performed each year, and the rate of retearing after two years is 11.0% to 94.0%.[4] Nearly half of the patients' postoperative pain persists without relief. Although surgical procedures have rapidly developed in recent years, repaired tissue rarely regains the natural ordered gradient histological structure, especially that of the typical fibrocartilage complex. Thus, tendon-bone insertion healing remains a substantial challenge in sports medicine.[6]

A limited understanding of the healing method of tendon-bone insertion injury is a key factor restricting its treatment. Various biological and mechanical factors drive and coordinate the repair process.[7-12] Among them, mechanical stimulation is an important factor in promoting tendon-bone insertion repair.[13] A review study by Osborne et al[14] showed that long-term fixation after rotator cuff injury can increase shoulder stiffness and cause bone loss, and the timing of rehabilitation training is particularly important for high-quality healing and the prevention of stiffness. Six weeks after rotator cuff injury, more aggressive passive and active activities can gradually begin, helping patients return to a satisfactory exercise level and ability to work. Animal experiments have also confirmed that appropriate mechanical stimulation is conducive to the regeneration of tendon-bone insertion healing.[15]

We first developed a mechanical stimulus scheme to evaluate how mechanical stimulation affects tendon-bone insertion healing. Bedi et al[16] pointed out that immediate mechanical stimulation after anterior cruciate ligament (ACL) reconstruction could cause macrophages to accumulate and aggravate the inflammatory response in tendon-bone insertion, interrupting tendon-bone insertion healing. Wada et al[17] found that excessive mechanical load after rotator cuff repair could delay the tendon-bone insertion healing process. Studies have confirmed that the inflammatory stage is a critical period that affects the quality of tendon-bone insertion healing. Excessive aggregation of inflammatory cells can cause increased fibrovascular scar tissue formation and make it difficult to reconstruct the histological structure of tendon-bone insertion. Lu et al[18] explored different exercise plans in a tendon-bone insertion repair model. They compared treadmill running initiated on postoperative days 2, 7, and 14, and found that postoperative treadmill running initiated on postoperative day 7 had a more prominent effect on tendon-bone insertion healing. Our pre-experiments also showed that treadmill running initiated on postoperative day 7 had a higher histomorphological score (Supplementary Figures aa and ab). Therefore, mechanical stimulation after the inflammatory period may avoid aggravating the inflammatory response and may be more conducive to tendon-bone insertion healing.[17-19] Previous studies have mostly focused on the relationship between mechanical stimulation and the fibrocartilage layer, while the effect of mechanical stimulation on tendon, fibrocartilage layer, and bone in the fibrocartilage complex is unclear.

We hypothesized that treadmill training starting after the inflammatory phase promotes repair of the fibrocartilage complex after tendon-bone insertion injury. The purpose of the present study was to compare tendon-bone insertion healing in mice subjected to treadmill training initiated on postoperative day 7 and free cage recovery, and to evaluate the quality of fibrocartilage complex repair, biomechanical properties, and motor function.

Methods

This study was reviewed and approved by the Animal Ethics Committee of our university. All animal studies have been checked in accordance with the ARRIVE guidelines. Breeding and operating of all animals were conducted in accordance with standard processes and guidelines.

Study design. A total of 92 eight-week-old male C57BL/6 mice were purchased from the Animal Centre of the First Affiliated Hospital of Army Medical University and housed four mice per cage. These animals had similar anatomical structures and pathophysiological processes after Achilles tendon-bone insertion injury. All mice underwent Achilles tendon-bone insertion injury and repair surgery, and were divided into six groups by the random digital table method as follows: Control group-1 month (1 M-C), Control group-2 months (2 M-C), Control group-3 months (3 M-C), Training group-1 month (1 M-T), Training group-2 months (2 M-T), and Training group-3 months (3 M-T). For each animal, one specific investigator (FW) administered the training based on the

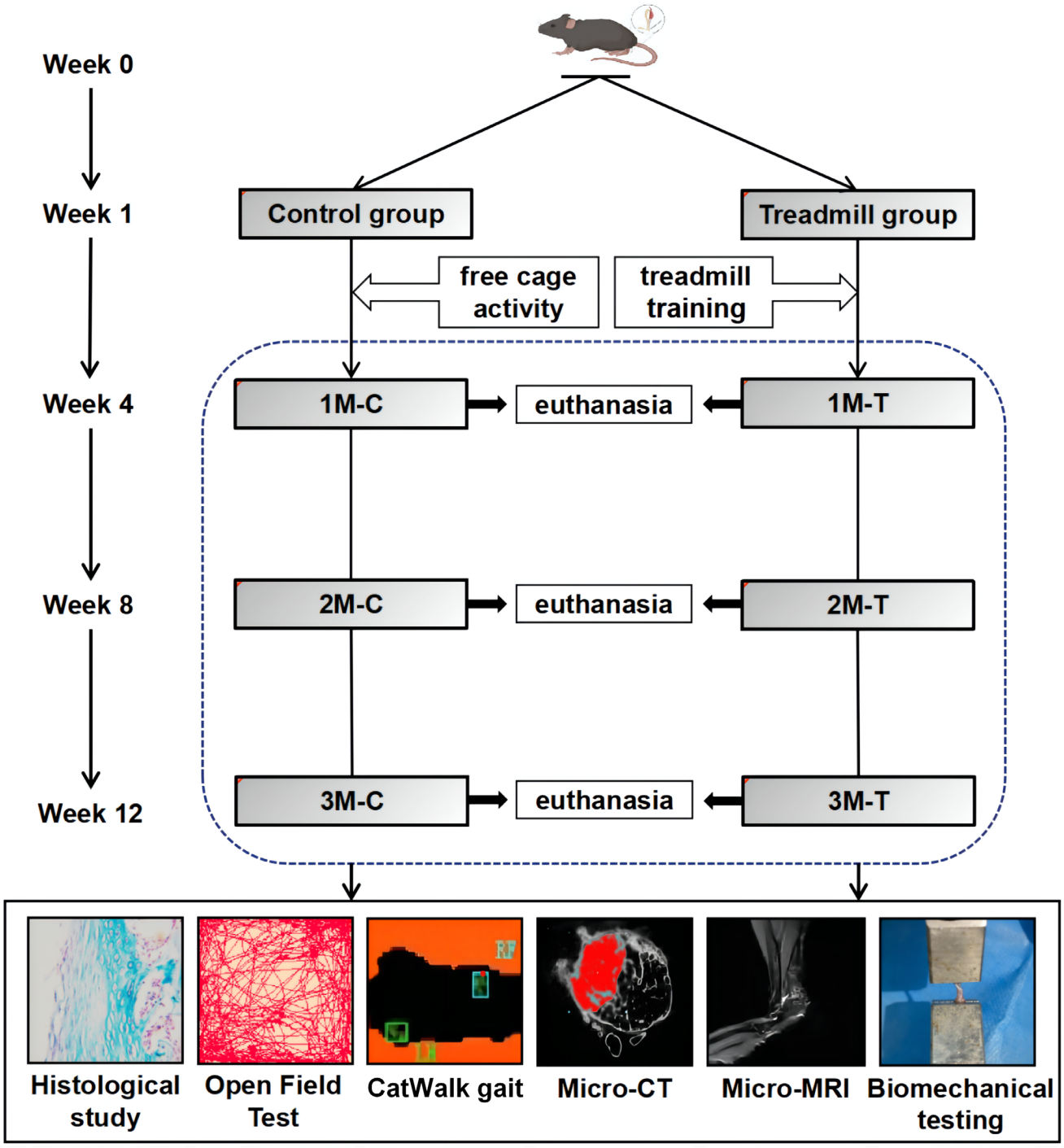

Fig. 1

A schematic diagram showing the entire experimental process.

randomization table. This investigator was the only person aware of the training group allocation. All mice were allowed free movement in the cage after the operation. The control group mice had full free activity in the cage, and the training group mice started the treadmill training one week after the surgery. Mice were euthanized at one month, two months, and three months after the surgery (Figure 1), and the number of animals used in each experiment is described in detail in the Results. A detailed protocol was prepared before the study.

Surgical procedures. All mice were injected in the right lower abdomen with 0.3% pentobarbital sodium anaesthetic (dose: 0.1 ml/10 g). Briefly, after sterile preparation of the entire forelimb, an approximately 5 mm

longitudinal incision was made at 2 mm on the right side of the calcaneus, and the soft-tissue was split to expose the insertion site of the Achilles tendon. The end of the Achilles tendon was fixed with 6-0 polydioxanone (PDS) suture (Ethicon, USA) in an "8" figure fashion, the Achilles tendon was sharply transected at its insertion on the surface of the calcaneus, and any fibrocartilage at the enthesis was scraped with a blade until cancellous bone was exposed. Then, a bone marrow needle was used to pierce the bone marrow from right to left at 2 mm below the calcaneus surface, and 6-0 PDS sutures were passed through the bone tunnel. The suture was tightened to approximate the Achilles tendon to its original footprint, and interrupted suturing was used to close the cutaneous incision (Supplementary Figures ba to bf).[20] Stress to failure of tendon-bone insertion in surgical model mice was validated (Supplementary Figures bg and bh).

Treadmill training. All mice were trained on adaptive treadmill training before surgery. The treadmill parameters were as follows: 5 to 10 m per minute, 20 minutes per day, five days per week, and a 0° tilt angle. The 1 M-T, 2 M-T, and 3 M-T groups began treadmill training on postoperative day 7 with the following treadmill training intensity and parameters: 10 m per minute, 30 minutes per day, five days per week, and a 0 tilt angle. The treadmill has eight runways with electric stimulators at the end of each runway. The voltage was set at 1.2 mAh. Up to four mice were allowed to run simultaneously per runway, and all mice were closely monitored during running. Training time was between 9.30am and 11.30am, and the training order was randomized daily, with each animal trained at a different track each test day. One experimenter (FW) was dedicated to treadmill training of the mice; only this experimenter knew the grouping of the mice (training group or control group) until all the experiments were completed.

Histological staining. Five mice were randomly selected in each group for histological staining. Part of the calcaneus and Achilles tendon was preserved to obtain complete tendon-bone insertion specimens, tendon-bone insertion specimens were fixed in 4% paraformaldehyde (Solarbio, China) for 48 hours, then decalcified in EDTA decalcifying solution (Solarbio) for 48 hours, and finally dehydrated in 30% paraformaldehyde-sucrose solution (Leagene, China) for 48 hours. Frozen specimens were cut in 7 μm thick sections in the sagittal plane by a microtome (LEICA CM1950, Germany). Frozen sections were stained with haematoxylin-eosin (H&E) (Solarbio) and Alcian blue (Solarbio) using standard procedures, and the specimens were stored at room temperature after staining. The stained tendon-bone insertion sections were analyzed by a Zeiss AxioVert microscope (Germany) equipped at 40× magnification, and the images were saved on the laboratory database.

Histomorphological score. Tendon-bone insertion healing maturity was evaluated using the scale developed by Ide et al[21] and Bian et al.[22] There were eight categories used for the evaluation based on H&E staining and Alcian blue staining. Overall, the scores were divided into the sum of various categories, with a value range of 0 to 24 points (Supplementary Table i). A higher score indicates better tendon-bone insertion healing maturity. When performing histological scoring, we first modified the histological scoring scale of the tendon-bone insertion according to the literature. The scale scoring system was then studied by two professionals (XL, XB), and after the study the same samples were scored, and formal scoring was started once the error rate of the scoring results had reached less than 5%. At the time of formal scoring, all samples were blinded to the observers, and after scoring was completed the mean score of the two was removed as the final histological score for that sample for statistical purpose.

Immunohistochemical staining and analysis. Three consecutive sections from each specimen were selected and rewarmed, rehydrated, placed in 3% bovine serum albumin (BSA), and incubated at 37°C for 30 minutes to block non-specific binding. Subsequently, 0.1% Triton X-100 was added, and the sections were incubated at 37°C for 20 minutes to increase cell permeability. Primary antibodies against type II collagen (COL2A1) (1:200; Abcam, USA) and SOX9 (1:200; Abcam) were added, and the samples were incubated at 4°C overnight. The next day, the sections were washed with 0.01 mol/l phosphate-buffered saline (PBS), secondary antibodies were added, and the sections were incubated at 37°C for two hours, soaked in PBS for five minutes, and stained with 3,3'-Diaminobenzidine (DAB) and haematoxylin. The sections were mounted using neutral resins. All the stained sections were viewed and photographed under a Zeiss AxioVert microscope. Cells positive for the targeted proteins were counted at a magnification of 40× in three fields of each slide. The positive cell numbers were normalized to the cell number per 100 total cells.

RNA isolation and quantitative real-time polymerase chain reaction. The tendon-bone insertion tissue specimens were cut into pieces, and the total RNA in the samples was extracted by TRIzol reagent (Thermo Fisher Scientific, USA). Quantitative polymerase chain reaction (PCR) was performed on total complementary DNA (cDNA) with PrimeScript RT Master Mix (Takara, Japan), and mouse-specific primers using the Thermal Cycler Dice Real-Time System (Takara) at 95°C for ten seconds, followed by 40 cycles of 95°C for five seconds and 60°C for 30 seconds. Relative gene expression was quantified by densitometry and normalized to the expression of the housekeeping gene glyceraldehyde 3-phosphate dehydrogenase (GAPDH). The sequences of COL2A1, type X collagen (COL10A1), SOX9, and GAPDH gene primers used in our experiments are listed in Supplementary Table ii.

Western blotting. Tendon-bone insertion tissues were cut into pieces, and radioimmunoprecipitation assay (RIPA) lysis buffer was added to lyse the tissue on ice. The protein concentration was measured using a BCA Protein Assay kit (Beyotime, China), and the protein samples were separated by 12% SDS-polyacrylamide

gel electrophoresis (SDS–PAGE), transferred onto polyvinylidene difluoride (PVDF) (Merck, USA) membranes, and incubated with 5% bovine serum albumin (Solarbio) for one hour. The primary antibodies were added to the PVDF membranes and incubated at 4°C overnight. Primary antibodies included COL2A1 (1:1,000, Abcam), COL0A1 (1:1,000, Abcam), SOX9 (1:1,000, Abcam), and β-actin (1:5,000, Abcam). Then, the membranes were incubated with horseradish peroxidase (HRP)-conjugated secondary antibodies (Beyotime) at 37°C for two hours. Finally, the reaction solution was added for the exposure analysis.

Micro-MRI and micro-CT. Tendon-bone insertion specimens were taken with an intact calcaneus, and we preserved a portion of the tendon tissue at the tendon end of the tendon-bone insertion in order to ensure the structural integrity of the tissue at the tendon-bone insertion. The specimens were fixed in 4% paraformaldehyde (Solarbio). Micro-CT was performed using a Skyscan1276 radiograph Microtomograph (Micro CT) instrument (Bruker, USA) with the following parameter settings: voltage 55 kV, current 200 μA, scan resolution 9.8 μm, and visual field size 2,016 × 1,304. The results were analyzed using Scanner software for Type Skyscan 1276 Micro CT (Bruker, Germany), and the area of interest was selected on the axial image. Tendon insertion into the proximal heel of the bone marrow canal was identified as the region of interest, and the bone volume/total volume (BV/TV), trabecular thickness (Tb. Th), trabecular number (Tb. N), and bone mineral denisty (BMD) were evaluated.

The quality of tendon-bone insertion healing and repair was assessed using micro-MRI in each group. Mice were maintained under anaesthesia with 2% isoflurane in a 1:1 mixture of O_2:N_2O. Images were obtained using a 9.4 T/160 mm animal MRI system (Agilent Technologies, USA). Radiofrequency excitation and signal detection were accomplished with a 72 mm quadrature volume coil and a four-channel phased-array coil. The imaging protocol included T2-weighted coronal images.

Biomechanical testing. ElectroForce Mechanical Test Instruments (TA Instruments, USA) were used to detect the stress to failure (N) of all samples. The Achilles tendon-bone insertion connection specimen was removed and placed in a 1× PBS petri dish in an icebox for testing. The sample was fixed with cyanoacrylate adhesive and fixed to the tensile instrument, and biomechanical tests were conducted at room temperature. First, a 0.05 N preload was applied for one minute, and then the specimen was stretched at 0.03 mm/second to ensure consistency in measuring process times. Data involving tendon or foot terminal slip and fracture of non-tendon-bone insertion connections were excluded.

CatWalk gait analysis and open field test. The static and dynamic gait parameters of the mice were analyzed by the CatWalk system.[23] The mice were placed at one end of the CatWalk glass plate channel in dark and quiet surroundings. The mice were allowed to continuously run to the other end and returned to their cages after completing three trips. The channel glass plate bottom emitted and reflected green light. When the mouse paw made contact with the glass plate, the green light was refracted and recorded. The brightness of the green signal increased as the foot weight increased. A high-speed camera was installed directly under the glass plate for image photography and capture.

The open-field test was conducted in quiet and lit rooms consisting of four (40 cm × 40 cm × 30 cm) square activity rooms, and intelligent video tracking software EthoVision 11.0 (Noldus, the Netherlands) was placed elevated above the centre of the room according to Bian et al.[22] Mice were acclimated in the environment for five minutes before the test. One mouse experiment per activity room was conducted, and the rooms were cleaned with 75.0% alcohol before testing. The alcohol was allowed to evaporate completely prior to the test to avoid adverse reactions to the smell; the mice were gently placed in the room, and the button was clicked to start the intelligent software. The mice were continuously observed for 30 minutes, and intelligent video tracking software was used to record their movement by a continuous sampling method, including movement route, distance, and speed.

Statistical analysis. Data are presented as the mean and standard deviation (SD). The independent-samples *t*-test and one-way analysis of variance (ANOVA) were used for comparisons between two groups and among multiple groups, respectively. Model assumptions were checked using the Shapiro-Wilk normality test and Levene's test for homogeneity of variance and by visual inspection of residual and fitted value plots. Differences were considered significant when $p < 0.05$. The statistical analysis was performed using SPSS v25.0 software (IBM, USA).

Results

Histomorphometric analysis. Frozen tendon-bone insertion sections were subjected to Alcian blue (Figure 2a) and H&E staining (Supplementary Figure ad), and tendon-bone insertion healing maturity was assessed using the histomorphological score scale (Supplementary Table i). The results showed that the training group had better healing quality, and the histomorphological scores of the 1 M-T, 2 M-T, and 3 M-T groups were significantly higher than those of the 1 M-C, 2 M-C, and 3 M-C groups (Figure 2b). Table I and Supplementary Table iii demonstrate the histomorphological score for each item, indicating that treadmill training can promote tendon-bone insertion repair. We found that the mean weight in the training group was significantly lower than that in the control group at two and three month (Figure 2c).

Immunohistochemical assessments. Quantitative analysis of immunohistochemical staining (Figure 3a) showed that the percentages of COL2A1- and SOX9-positive cells in the 1 M-T, 2 M-T, and 3 M-T groups were significantly higher than those in the 1 M-C, 2 M-C, and 3 M-C groups (Figures 3b and 3c).

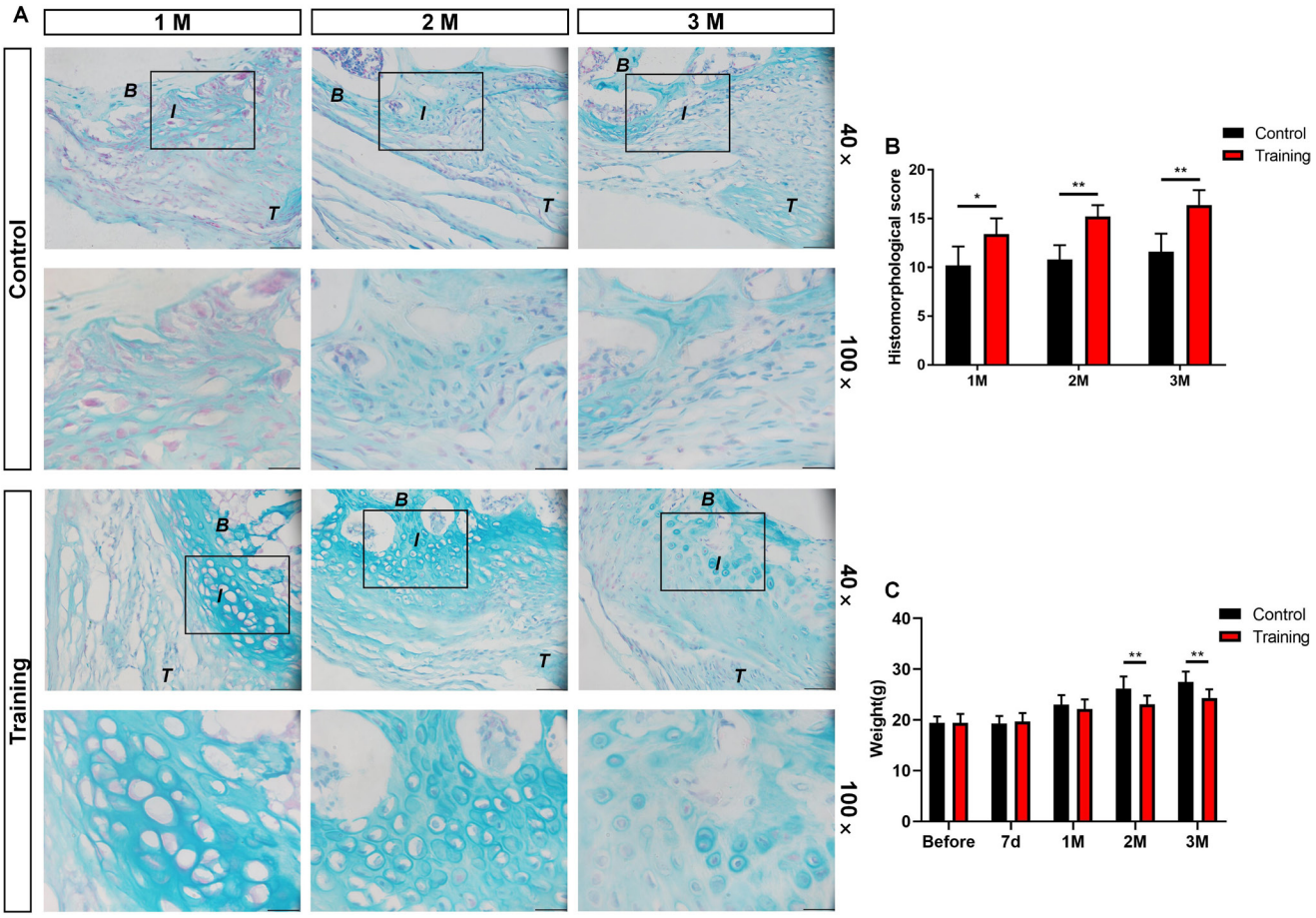

Fig. 2

Tendon-bone insertion healing quality significantly improved after treadmill training. a) Representative Alcian staining images of each group. b) Histomorphological score of each group. c) Statistics of each group of mouse body weight changes. Scale bars indicate 50 μm for 40× magnification and 20 μm for 100× magnification. Data are shown as the mean and standard deviation. N = 5 for all groups, *p < 0.05, **p < 0.01 compared with the control groups. B, bone area; I, insertion area; T, tendon area.

Table I. Mean histomorphological score and standard deviation for each item of each group (n = 5 for all).

Group	Fibrocartilage cell number	Fibrocartilage cell alignment	Collagen fibre continuity	Collagen fibre orientation	Tidemark	Cellularity	Vascularity	Inflammation	Total scores
1 M-C	1.00 (0.63)	1.20 (0.40)	1.40 (0.49)	1.00 (0.63)	0.60 (0.49)	1.40 (0.49)	1.80 (0.40)	1.80 (0.40)	10.20 (1.94)
1 M-T	1.80 (0.40)*	1.60 (0.49)	1.40 (0.49)	1.40 (0.49)	1.40 (0.49)†	1.80 (0.40)	2.20 (0.40)	1.80 (0.40)	13.40 (1.62)†
2 M-C	1.20 (0.40)	1.60 (0.49)	1.00 (0.00)	1.00 (0.00)	0.80 (0.40)	1.20 (0.40)	2.60 (0.49)	1.40 (0.49)	10.80 (1.47)
2 M-T	1.80 (0.75)	1.60 (0.49)	1.60 (0.49)	1.60 (0.49)	2.00 (0.00)‡	1.60 (0.49)	2.80 (0.40)	2.20 (0.40)‡	15.20 (1.17)‡
3 M-C	1.40 (0.49)	0.80 (0.40)	1.60 (0.49)	1.20 (0.40)	0.60 (0.49)	1.80 (0.40)	2.80 (0.40)	1.40 (0.49)	11.60 (1.85)
3 M-T	2.00 (0.00)*	2.40 (0.49)*	1.80 (0.40)	1.60 (0.49)	1.60 (0.49)*	2.20 (0.40)	3.00 (0.00)	2.00 (0.00)*	16.40 (1.50)*

*Statistical difference compared with 3 M-C.
†Statistical difference compared with 1 M-C.
‡Statistical difference compared with 2 M-C.
C, control; M, months; T, training.

Gene and protein expression analysis. Both reverse transcription (RT)-PCR (Figure 4a) and Western blot (Figures 4b and 4c) analyses showed that the messenger RNA (mRNA) and protein expression levels of the COL2A1 and SOX9 genes were significantly increased in the 1 M-T, 2 M-T, and 3 M-T groups compared with those in the control group. The protein expression of COL10A1 in training group was significantly higher only at two and three months.

Micro-MRI and micro-CT analysis. Our results obtained by micro-MRI analysis show that the 1 M-T, 2 M-T, and 3 M-T groups had better continuity, a stronger signal intensity, better thickness, and formed less scar tissue (Figure 5a). Micro-CT scans of the tendon-bone insertion showed

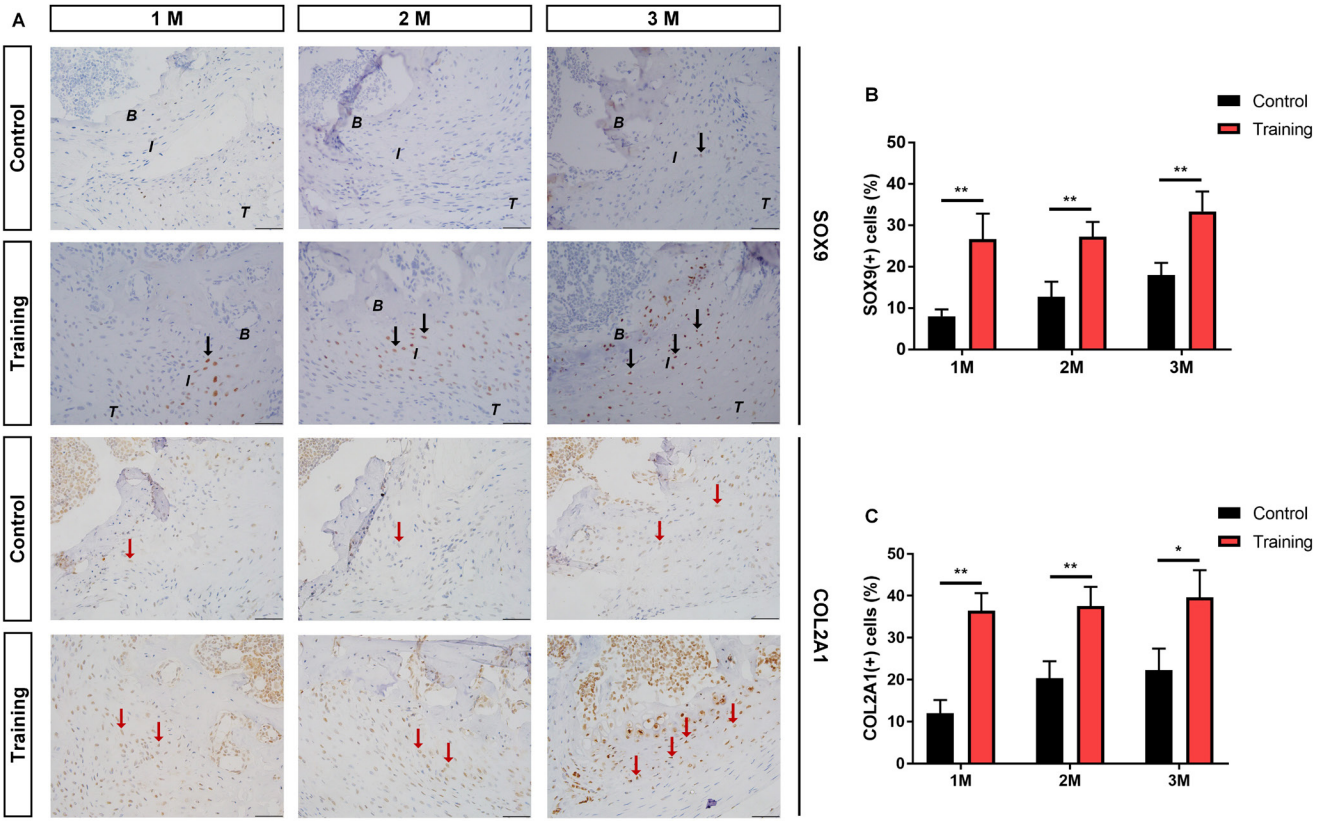

Fig. 3

Treadmill training promotes type II collagen (COL2A1) and SOX9 protein expression at the interface of tendon-bone insertion. a) Representative immunohistochemical staining images of each group. b) Quantitative analysis of the proportion of SOX9-positive cells. c) Quantitative analysis of the percentage of COL2A1-positive cells. Scale bar: 50 μm, Magnification: 40×. Black arrows indicate the SOX9-positive, and red arrows indicate COL2A1-positive cells. Data are shown as the mean and standard deviation. N = 3 for all groups, *p < 0.05 and **p < 0.01 compared with the control groups. B, bone area; I, insertion area; T, tendon area.

that the BMD values of the 1 M-T, 2 M-T, and 3 M-T groups were significantly higher than those of the 1 M-C, 2 M-C, and 3 M-C groups, and the BV/TV was significantly increased at 2 M-T and 3 M-T. While Tb.Th and Tb.N showed some increasing trend, they were not statistically significant compared to the control group (Figures 5b and 5c). Micro-CT raw data are shown in Supplementary Table iv.

Open field test and CatWalk gait analysis. The open-field test revealed that treadmill training significantly improved the autonomic movement ability of the model mice and enhanced performance, as demonstrated by the faster movement speed and longer distance travelled compared with the control group (Figures 6a and 6b). CatWalk gait analysis results found that the training group significantly increased the average speed, swing speed, and stride length of the model mice compared with those of the control group mice . Meanwhile, the training group model mice had a shorter stand time during walking (Figures 6c and 6d).

Biomechanical analysis. We performed complete biomechanical testing of the tendon-bone insertion. We found that the stress to failure of the 3 M-T group was significantly higher than that of the 3 M-C group (Figure 6e). Therefore, we deduced that treadmill training can aid in the repair of the fibrocartilage complex and enhance the local biomechanical strength.

Discussion

Our results show that treadmill training initiated on postoperative day 7 improves many aspects of tendon-bone insertion healing, including higher tendon-bone insertion histological maturity, better fibrocartilage complex remodelling, and increased neonatal bone penetration. Functionally, these improvements manifested as better tendon-bone insertion biomechanical properties and stronger sports ability, which became more pronounced over the exercise time period. Although only male mice were used in our study, this does not affect the generalization of the findings. On the one hand, the estrus period and menstrual period caused by oestrogen secretion in female mice may become a tricky variable affecting the experimental data. On the other hand, the mechanical stimulation produced by treadmill training was the only intervention factor in our study. Oestrogen levels may have some effect on individual responses to mechanical stimuli, but do not affect the overall trend. Therefore, we believe that our results are also instructive for females.

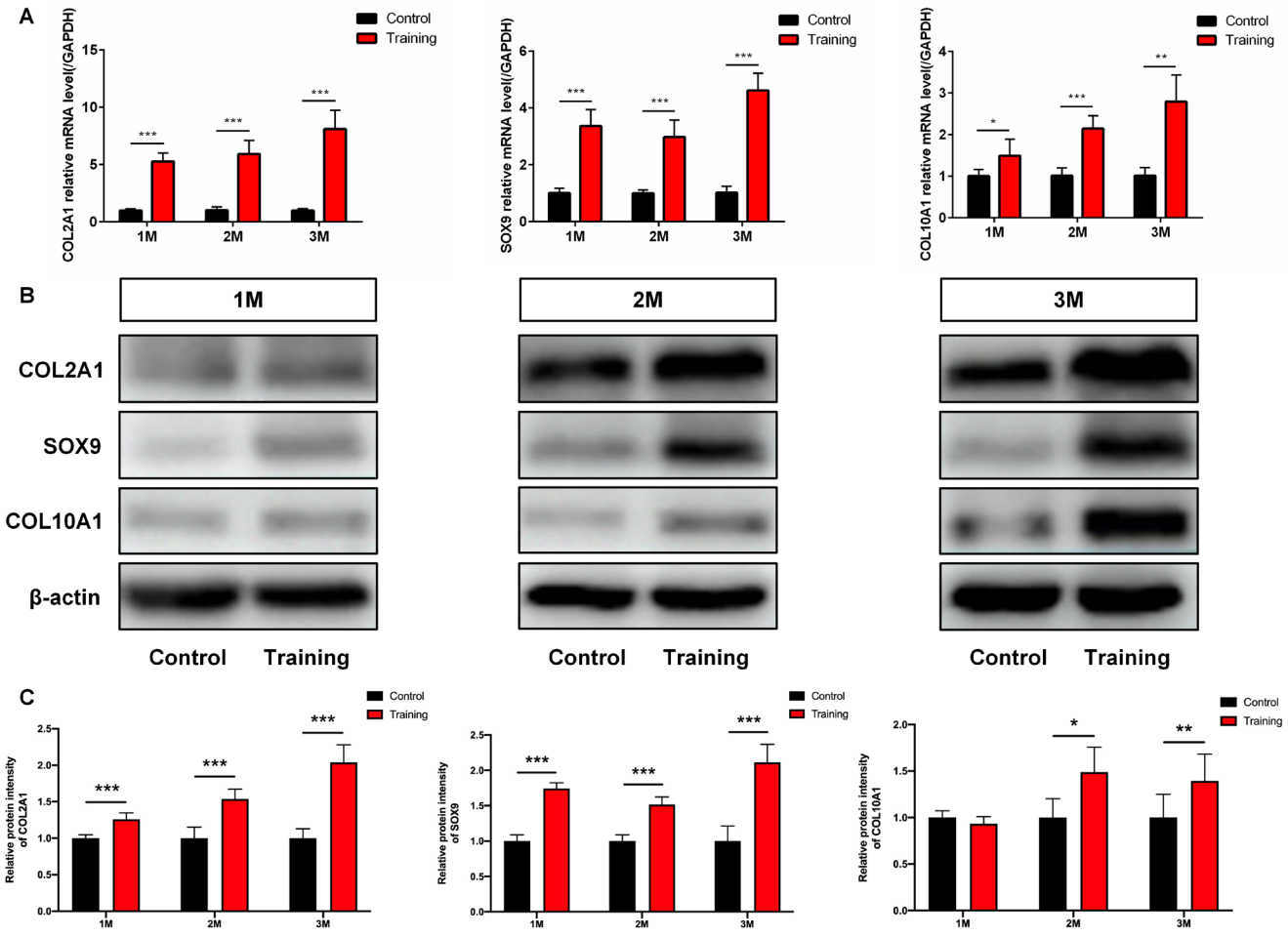

Fig. 4

The expression of cartilage markers in the tendon-bone insertion samples was significantly increased after treadmill training. a) The messenger RNA (mRNA) expression levels of cartilage markers such as type II collagen (COL2A1), SOX9, and type X collagen (COL10A1) in each group. b) Typical Western blot (WB) bands of cartilage markers of each group. c) Mean grey value statistics of WB bands in each group. Data are shown as the mean and standard deviation. N = 5 for all groups, *p < 0.05, **p < 0.01, and ***p < 0.001 compared with the control groups. GAPDH, glyceraldehyde 3-phosphate dehydrogenase.

These results suggest that mechanical stimulation can promote the healing process of tendon-bone insertion injury, and that seven days of delayed mechanical stimulation is beneficial for tendon-bone insertion healing, consistent with the mainstream views in the current literature. Tendon-bone insertion healing, in general, like tendon healing, follows a typical wound-healing course: a short inflammatory phase (lasting on the order of days) is followed by a proliferative phase (lasting on the order of weeks), which in turn is followed by a remodelling phase (lasting on the order of months). Our pre-experiment study has confirmed that mRNA expression levels of IL-1β, IL-6, and TNF-α at the tendon-bone insertion were significantly elevated on postoperatives day 1 and 3, which was in the phase of acute inflammation, while IL-1β, IL-6, and TNF-α mRNA expression levels decreased significantly on postoperative day 7 (Supplementary Figure ac), indicating that the acute inflammatory phase had passed. Therefore, day 7 was chosen to start treadmill training. Among the literature, Bedi et al[16] argued that delayed mechanical loading better promotes tendon-bone insertion healing after anterior cruciate ligament reconstruction, possibly by alleviating postoperative acute inflammation. Packer et al[24] pointed out that postoperative delayed load is more helpful for mineral deposits and new bone ingrowth at the epiphysis of tendon-bone insertion. Lu et al[18] found that compared with treadmill running started on postoperative day 2 and full free activity, treadmill running that started on postoperative days 7 and 14 was more helpful for the histological maturation of tendon-bone insertion healing, and improved osteogenic and chondrogenic gene expression, along with higher bone volume fractions and failure loads, suggesting that delayed mechanical load is more helpful for tendon-bone insertion healing.

Most studies suggest that the key to tendon-bone insertion healing lies in the regeneration of the fibrochondral layer, including non-calcified fibrocartilage cells and calcified fibrocartilage cells, and the type II and type X collagen fibres secreted by the cells.[25–27] However,

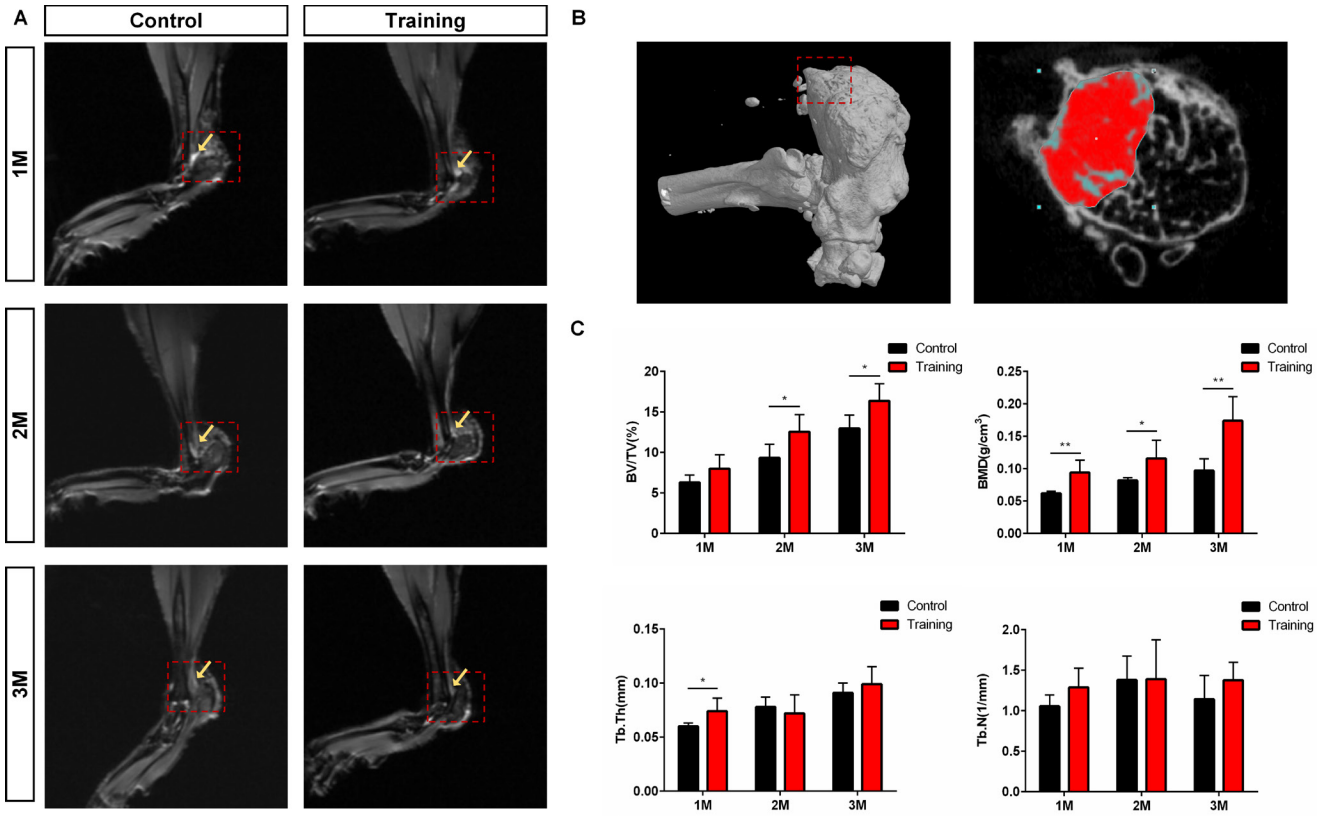

Fig. 5

Treadmill training promotes new bone penetration at the tendon-bone insertion and enhances bone density. a) Coronal T2-weighted image showing tendon-bone insertion; the red box indicates the tendon-bone insertion, and the yellow arrow shows the high signal area. b) The red box indicates the Achilles tendon insertion (footprint area) on the left image, and region of interest (the red area on the right image) in microCT analysis. c) The mean bone volume/total volume (BV/TV), trabecular bone thickness (Tb.Th), trabecular bone number (Tb.N), and bone mineral density (BMD) value of each group were measured. N = 5 for all groups. *p < 0.05, **p < 0.01 compared with the control groups.

anatomical observations of tendon-bone insertion show that it contains four layers, comprising tendon, non-calcified fibrocartilage, calcified fibrocartilage, and bone. The four-layer structure forms an orderly fibrocartilage complex according to their respective biological and mechanical properties, and the fibrocartilage complex is an important structure of tendon-bone insertion.[28,29] The fibrocartilage complex structure and function are challenging to regain after injury. Therefore, structural reconstruction of the fibrocartilage complex is a critical aspect of tendon-bone insertion damage repair.

Tendons in the fibrocartilage complex are pure dense fibrous connective tissue arranged in parallel into the non-calcified fibrocartilage, which is mainly composed of fibroblasts and type I collagen.[30] Schwartz et al[31] and Thomopoulos et al[32] showed that reduced muscle load impaired the maturation of tendon-bone insertion and resulted in disordered collagen fibre angular distribution within the fibre cartilage, leading to a significant increase in the angular deviation of collagen fibre distribution. Our histological staining results showed that the collagen fibres in the tendon-bone insertion group were more orderly after treadmill training; however, no significant differences were found between groups. In addition, the training group had fewer vessels and a lower inflammatory response than the control group. Our results showed that mechanical stimulation after the inflammatory phase during healing can help to reduce scar formation and reshape the optimal collagen fibre arrangement in tendon-bone insertion to restore normal structure, which we confirmed by MRI.

The fibrocartilage layer of the tendon-bone insertion includes non-calcified fibrocartilage and calcified fibrocartilage. A previous study showed that this layer is the core structure of the fibrocartilage complex.[33] Our results showed that the histological score of the fibrocartilage cell number and fibrocartilage cell alignment in the training group was significantly higher than that in the control group at postoperative month 3. Meanwhile, to further confirm this finding, PCR, WB, and immunohistochemistry were carried out to detect the expression of chondrogenic genes at both the mRNA and protein levels. The results confirmed that expression of COL2A1 and SOX9 was significantly upregulated in the training group compared with the control group at every time-point. Similar results were found in previous research: Tian et al[34] showed that mesenchymal stem cells (MSCs) are the main cells involved in tendon-bone insertion

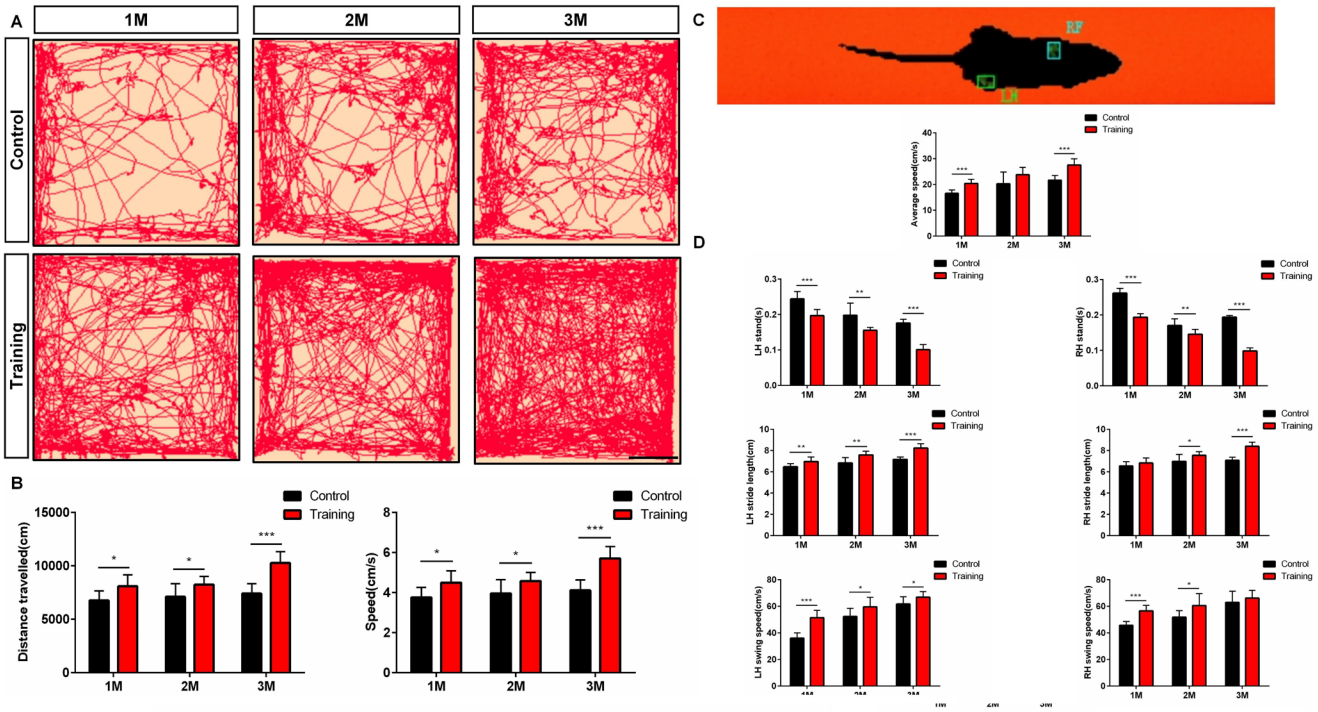

Fig. 6

Treadmill training enhanced the motor function and biomechanical strength of the tendon-bone insertion. a) Performance in the open-field test and the results of each group, the red lines indicate trajectories of mice. b) The distance travelled and speed of each group were measured. Scale bar: 10 cm. c) Representative test image of the CatWalk gait, and the green box indicates the footprints. d) The mean speed, swing speed, stride length, and stand time of each group were recorded with standard deviations. *p < 0.05, **p < 0.01, and ***p < 0.001 compared with the control groups.

injury repair and participate in damage repair through differentiation into osteocytes, chondrocytes, tenocytes, and myofibroblasts. Masuda et al[35] confirmed in vitro that mechanical stimulation can regulate chondrogenic differentiation, in which the size, type, and time of action differ in the regulation of chondrogenic differentiation. Physiologically, tendon-bone insertion is subject to multiple biomechanical effects and can be stimulated by pressure stress and tension stress during treadmill training, which may be the cause of increased chondrocytopiesis in tendon-bone insertion. All these previous studies, along with our results, suggest that mechanical stimulation after the inflammatory phase plays a positive role in the reshaping of fibrocartilage during tendon-bone insertion repair, which is possibly related to mechanical stimulation promoting chondrogenic differentiation of MSCs.

In addition, the tidemark forms the boundary between non-calcified fibrocartilage and calcified fibrocartilage, and can be considered the threshold of tissue absorption of minerals. The results of the current study suggest that the re-emergence of tidemarks is an important standard marker of good fibrocartilage layer reconstruction. This study also showed that histological tidemark scores were significantly higher in the training group than in the control group at postoperative months 1, 2, and 3, and a significant tidemark was observed in some samples in the training group. Juncosa-Melvin et al[36] reported that mechanical stimulation improves extracellular matrix expression and enhances tissue stiffness and hardness. In vitro studies have similarly shown that when cells in tissues are subjected to mechanical stimulation, the extracellular matrix is usually deposited in the direction of the mechanical stimulation. We propose that treadmill training for mechanical stimulation of the tendon-bone insertion promoted mineral deposition within the injury region, promoting reconstruction that resembled the normal extracellular matrix components and proportions of tendon-bone insertion, in turn producing tidemarks.

The bone tissue of the tendon-bone insertion is critical for insertion attachment. During tendon-bone insertion repair, mineralized matrix deposition and bone absorption balance are disrupted.[37] Osteolysis at the tendon-bone insertion can impair pullout strength during tendon-bone healing and lead to surgery failure. Feng et al[38] confirmed that BMMSC^{scx}-exos or miR-6924-5p improve the quality of tendon-bone healing by inhibiting osteolysis. Galatz et al[39] reported that delayed rotator cuff fracture repair results in reduced bone density at the tendon-bone insertion. Mechanical load is a key regulator of bone transformation in the human body. Previous studies have shown that fixation after tendon-bone insertion injury increases bone resorption rates, while increasing local load can stimulate bone formation and increase bone density.[40,41] This study showed that the BV/TV and BMD were significantly higher at postoperative months 2 and 3 in the training group than in the control

group, and partial improvement in bone Tb.N and Tb.Th was observed, suggesting that treadmill training can stimulate new bone generation and improve bone density. In addition, partial improvements in Tb.N and TB.Th suggest that treadmill training can stimulate new bone generation in tendon-bone insertion and improve bone density to improve healing strength and function, largely consistent with previous reports.[18,19]

The tendon-bone insertion transmits force from the tendon to the bone, playing a vital role in bodily activities. Therefore, its functional recovery after injury is the ultimate clinical goal.[42] First, we used a biomechanical test to examine the biomechanical properties of the tendon-bone insertion. Our results show that the failure load strength of the training group was significantly higher than that of the control group. Furthermore, we used CatWalk gait analysis and the open-field test to analyze the motor ability of the mice. CatWalk gait analysis is considered an effective method for assessing above-ground motor function in small animals such as rodents, and the open-field test reflects autonomous motor behaviour and exploratory behaviour in mice.[43,44] In our study, these two tests were performed to examine the instantaneous and sustained motion capacity. The CatWalk gait analysis results showed that the training group had better mean speed, swing speed, stride length, and stand time than the control group. In addition, the distance travelled and the speed in the open-field test were greater in the training group than in the control group, and the effect became obvious as the time of the treadmill training was extended, suggesting that treadmill training substantially improves the motor function level after tendon-bone insertion healing, which has theoretical guiding significance for clinical rehabilitation.

The most important aim of our results is to achieve clinical translation; although the anatomy of mice tendon-bone insertion is closest to that of humans among mammals, considering the obvious individual differences in clinical patients, standardized treadmill training similar to mice cannot be achieved, and treadmill training programmes need to weigh a variety of factors. Therefore, the development of treadmill training programmes that meet the individual clinical patients needs in-depth research, and our results have important implications for the development of treadmill training regimens at the appropriate timing and intensity for clinical patients.

This study has the following limitations. First, the expected model effect of our study can be achieved, but whether this treadmill scheme is optimal needs to be confirmed with additional studies on the optimal gradient. Second, we have not elucidated the specific molecular mechanisms by which this protocol promotes healing of tendon-bone insertion; however, we have screened associated genes using a transcriptomic sequencing approach, and we will study these genes in the future. Third, the mouse model we constructed differs from the clinical human body. The above limitations also give us a lot of inspiration for future research. First, the training programme needs to be further refined in mouse models, including the start and end time, as well as the speed and slope, so as to better fit the clinical setting. Second, we need to further investigate the molecular mechanism of treadmill training to promote tendon-bone insertion healing. We are conducting research on the above two points. Finally, large animal experiments should be conducted, which will help to accelerate clinical translation. Nevertheless, this study provides information regarding clinical rehabilitation methods, including the timing and choice of strength.

In conclusion, our results show that treadmill training regimens of 10 m per minute, 30 minutes per day, and five days per week on postoperative day 7 can promote structural remodelling of the fibrocartilage complex. We simulated clinical rehabilitation treadmill training, and the results might provide subsequent guidance for clinical rehabilitation training programmes.

Supplementary material

Figures showing typical haematoxylin and eosin-stained images and proinflammatory factor messenger RNA expression levels at different times after surgery, surgical procedures and biomechanical test of Achilles tendon detachment and repair, and setting for the biomechanical test and results of maximal stress to failure. Tables showing histomorphometric scoring system for tendon-bone insertion healing, target gene sequence list, scores for each item in the histomorphometric scoring system for each sample, and micro-CT raw data of tendon-bone insertion healing. An ARRIVE checklist is also included to show that the ARRIVE guidelines were adhered to in this study.

References

1. **Ponkilainen V**, **Kuitunen I**, **Liukkonen R**, **Vaajala M**, **Reito A**, **Uimonen M**. The incidence of musculoskeletal injuries: a systematic review and meta-analysis. *Bone Joint Res.* 2022;11(11):814–825.
2. **Atesok K**, **Fu FH**, **Wolf MR**, **et al**. Augmentation of tendon-to-bone healing. *J Bone Joint Surg Am.* 2014;96-A(6):513–521.
3. **Tashjian RZ**. Epidemiology, natural history, and indications for treatment of rotator cuff tears. *Clin Sports Med.* 2012;31(4):589–604.
4. **Colvin AC**, **Egorova N**, **Harrison AK**, **Moskowitz A**, **Flatow EL**. National trends in rotator cuff repair. *J Bone Joint Surg Am.* 2012;94-A(3):227–233.
5. **Brown TD**, **Johnston RC**, **Saltzman CL**, **Marsh JL**, **Buckwalter JA**. Posttraumatic osteoarthritis: a first estimate of incidence, prevalence, and burden of disease. *J Orthop Trauma.* 2006;20(10):739–744.
6. **Derwin KA**, **Galatz LM**, **Ratcliffe A**, **Thomopoulos S**. Enthesis repair: Challenges and opportunities for effective tendon-to-bone healing. *J Bone Joint Surg Am.* 2018;100-A(16):e109.
7. **Schulze-Tanzil GG**, **Delgado-Calcares M**, **Stange R**, **Wildemann B**, **Docheva D**. Tendon healing: a concise review on cellular and molecular mechanisms with a particular focus on the Achilles tendon. *Bone Joint Res.* 2022;11(8):561–574.
8. **Galatz L**, **Rothermich S**, **VanderPloeg K**, **Petersen B**, **Sandell L**, **Thomopoulos S**. Development of the supraspinatus tendon-to-bone insertion: localized expression of extracellular matrix and growth factor genes. *J Orthop Res.* 2007;25(12):1621–1628.
9. **Thomopoulos S**, **Williams GR**, **Gimbel JA**, **Favata M**, **Soslowsky LJ**. Variation of biomechanical, structural, and compositional properties along the tendon to bone insertion site. *J Orthop Res.* 2003;21(3):413–419.

10. **Wu Y**, **Shao Y**, **Xie D**, **et al**. Effect of secretory leucocyte protease inhibitor on early tendon-to-bone healing after anterior cruciate ligament reconstruction in a rat model. *Bone Joint Res.* 2022;11(7):503–512.
11. **Park J**, **Jo S**, **Lee M-K**, **Kim T-H**, **Sung I-H**, **Lee JK**. Comparison of ligamentization potential between anterior cruciate ligament-derived cells and adipose-derived mesenchymal stem cells reseeded to acellularized tendon allograft. *Bone Joint Res.* 2022;11(11):777–786.
12. **Park TJ**, **Park SY**, **Cho W**, **et al**. Developmental endothelial locus-1 attenuates palmitate-induced apoptosis in tenocytes through the AMPK/autophagy-mediated suppression of inflammation and endoplasmic reticulum stress. *Bone Joint Res.* 2022;11(12):854–861.
13. **Thomopoulos S**, **Kim H-M**, **Rothermich SY**, **Biederstadt C**, **Das R**, **Galatz LM**. Decreased muscle loading delays maturation of the tendon enthesis during postnatal development. *J Orthop Res.* 2007;25(9):1154–1163.
14. **Osborne JD**, **Gowda AL**, **Wiater B**, **Wiater JM**. Rotator cuff rehabilitation: current theories and practice. *Phys Sportsmed.* 2016;44(1):85–92.
15. **Dolkart O**, **Kazum E**, **Rosenthal Y**, **et al**. Effects of focused continuous pulsed electromagnetic field therapy on early tendon-to-bone healing. *Bone Joint Res.* 2021;10(5):298–306.
16. **Bedi A**, **Kovacevic D**, **Fox AJS**, **et al**. Effect of early and delayed mechanical loading on tendon-to-bone healing after anterior cruciate ligament reconstruction. *J Bone Joint Surg Am.* 2010;92-A(14):2387–2401.
17. **Wada S**, **Lebaschi AH**, **Nakagawa Y**, **et al**. Postoperative tendon loading with treadmill running delays tendon-to-bone healing: Immunohistochemical evaluation in a murine rotator cuff repair model. *J Orthop Res.* 2019;37(7):1628–1637.
18. **Lu H**, **Li S**, **Zhang T**, **et al**. Treadmill running initiation times and bone-tendon interface repair in a murine rotator cuff repair model. *J Orthop Res.* 2021;39(9):2017–2027.
19. **Zhang T**, **Chen Y**, **Chen C**, **et al**. Treadmill exercise facilitated rotator cuff healing is coupled with regulating periphery neuropeptides expression in a murine model. *J Orthop Res.* 2021;39(3):680–692.
20. **Shi Y**, **Kang X**, **Wang Y**, **et al**. Exosomes derived from bone marrow stromal cells (BMSCs) enhance tendon-bone healing by regulating macrophage polarization. *Med Sci Monit.* 2020;26:e923328.
21. **Ide J**, **Kikukawa K**, **Hirose J**, **et al**. The effect of a local application of fibroblast growth factor-2 on tendon-to-bone remodeling in rats with acute injury and repair of the supraspinatus tendon. *J Shoulder Elbow Surg.* 2009;18(3):391–398.
22. **Bian X**, **Liu T**, **Yang M**, **et al**. The absence of oestrogen receptor beta disturbs collagen I type deposition during Achilles tendon healing by regulating the IRF5-CCL3 axis. *J Cell Mol Med.* 2020;24(17):9925–9935.
23. **Kappos EA**, **Sieber PK**, **Engels PE**, **et al**. Validity and reliability of the CatWalk system as a static and dynamic gait analysis tool for the assessment of functional nerve recovery in small animal models. *Brain Behav.* 2017;7(7):e00723.
24. **Packer JD**, **Bedi A**, **Fox AJ**, **et al**. Effect of immediate and delayed high-strain loading on tendon-to-bone healing after anterior cruciate ligament reconstruction. *J Bone Joint Surg Am.* 2014;96-A(9):770–777.
25. **Lu H**, **Chen C**, **Qu J**, **et al**. Initiation timing of low-intensity pulsed ultrasound stimulation for tendon-bone healing in a rabbit model. *Am J Sports Med.* 2016;44(10):2706–2715.
26. **Lu H**, **Qin L**, **Cheung W**, **Lee K**, **Wong W**, **Leung K**. Low-intensity pulsed ultrasound accelerated bone-tendon junction healing through regulation of vascular endothelial growth factor expression and cartilage formation. *Ultrasound Med Biol.* 2008;34(8):1248–1260.
27. **Wong MWN**, **Qin L**, **Lee KM**, **Leung KS**. Articular cartilage increases transition zone regeneration in bone-tendon junction healing. *Clin Orthop Relat Res.* 2009;467(4):1092–1100.
28. **Lui P**, **Zhang P**, **Chan K**, **Qin L**. Biology and augmentation of tendon-bone insertion repair. *J Orthop Surg Res.* 2010;5:59.
29. **Martinek V**, **Latterman C**, **Usas A**, **et al**. Enhancement of tendon-bone integration of anterior cruciate ligament grafts with bone morphogenetic protein-2 gene transfer: a histological and biomechanical study. *J Bone Joint Surg Am.* 2002;84-A(7):1123–1131.
30. **Voleti PB**, **Buckley MR**, **Soslowsky LJ**. Tendon healing: repair and regeneration. *Annu Rev Biomed Eng.* 2012;14:47–71.
31. **Schwartz AG**, **Lipner JH**, **Pasteris JD**, **Genin GM**, **Thomopoulos S**. Muscle loading is necessary for the formation of a functional tendon enthesis. *Bone.* 2013;55(1):44–51.
32. **Thomopoulos S**, **Parks WC**, **Rifkin DB**, **Derwin KA**. Mechanisms of tendon injury and repair. *J Orthop Res.* 2015;33(6):832–839.
33. **Tits A**, **Plougonven E**, **Blouin S**, **et al**. Local anisotropy in mineralized fibrocartilage and subchondral bone beneath the tendon-bone interface. *Sci Rep.* 2021;11(1):16534.
34. **Tian F**, **Ji X-L**, **Xiao W-A**, **Wang B**, **Wang F**. CXCL13 promotes the effect of bone marrow mesenchymal stem cells (MSCs) on tendon-bone healing in rats and in C3HIOT1/2 cells. *Int J Mol Sci.* 2015;16(2):3178–3187.
35. **Masuda T**, **Takahashi I**, **Anada T**, **et al**. Development of a cell culture system loading cyclic mechanical strain to chondrogenic cells. *J Biotechnol.* 2008;133(2):231–238.
36. **Juncosa-Melvin N**, **Matlin KS**, **Holdcraft RW**, **Nirmalanandhan VS**, **Butler DL**. Mechanical stimulation increases collagen type I and collagen type III gene expression of stem cell-collagen sponge constructs for patellar tendon repair. *Tissue Eng.* 2007;13(6):1219–1226.
37. **Kekilli E**, **Ertem K**, **Yologlu S**, **Ceylan F**. Comparisons of the bone mineral density in dominant and nondominant forearm following clean-cut tendon injuries, repair, and passive mobilization. *J Clin Densitom.* 2006;9(2):198–201.
38. **Feng W**, **Jin Q**, **Ming-Yu Y**, **et al**. MiR-6924-5p-rich exosomes derived from genetically modified Scleraxis-overexpressing PDGFRα(+) BMMSCs as novel nanotherapeutics for treating osteolysis during tendon-bone healing and improving healing strength. *Biomaterials.* 2021;279:121242.
39. **Galatz LM**, **Rothermich SY**, **Zaegel M**, **Silva MJ**, **Havlioglu N**, **Thomopoulos S**. Delayed repair of tendon to bone injuries leads to decreased biomechanical properties and bone loss. *J Orthop Res.* 2005;23(6):1441–1447.
40. **Hettrich CM**, **Gasinu S**, **Beamer BS**, **et al**. The effect of mechanical load on tendon-to-bone healing in a rat model. *Am J Sports Med.* 2014;42(5):1233–1241.
41. **Hettrich CM**, **Gasinu S**, **Beamer BS**, **et al**. The effect of immobilization on the native and repaired tendon-to-bone interface. *J Bone Joint Surg Am.* 2013;95-A(10):925–930.
42. **Fealy S**, **Rodeo SA**, **MacGillivray JD**, **Nixon AJ**, **Adler RS**, **Warren RF**. Biomechanical evaluation of the relation between number of suture anchors and strength of the bone-tendon interface in a goat rotator cuff model. *Arthroscopy.* 2006;22(6):595–602.
43. **Navarro X**. Functional evaluation of peripheral nerve regeneration and target reinnervation in animal models: a critical overview. *Eur J Neurosci.* 2016;43(3):271–286.
44. **Seibenhener ML**, **Wooten MC**. Use of the Open Field Maze to measure locomotor and anxiety-like behavior in mice. *J Vis Exp.* 2015;96:52434.

Author information:
- J. Tan, MD, Orthopaedic Surgeon
- X. Liu, MD, Orthopaedic Surgeon
- M. Zhou, MD, Assistant Researcher
- F. Wang, MD, Orthopaedic Surgeon
- L. Ma, MD, Orthopaedic Surgeon
- H. Tang, MD, Assistant Researcher
- G. He, MD, Assistant Researcher
- X. Kang, MD, Orthopaedic Associate Professor
- X. Bian, MD, Orthopaedic Surgeon
- K. Tang, MD, Orthopaedic Professor

State Key Laboratory of Trauma, Burn and Combined Injury, Department of Orthopaedics/Sports Medicine Center, First Affiliated Hospital of Army Medical University, Chongqing, China.

Author contributions:
- J. Tan: Conceptualization, Investigation, Data curation, Formal analysis, Methodology, Writing – original draft.
- X. Liu: Investigation, Methodology, Software.
- M. Zhou: Methodology.
- F. Wang: Methodology.
- L. Ma: Investigation.
- H. Tang: Validation.
- G. He: Software.
- X. Kang: Software.
- X. Bian: Conceptualization, Methodology, Software, Writing – review & editing.
- K. Tang: Conceptualization, Funding acquisition, Resources, Writing – review & editing.

- X. Bian and K. Tang contributed equally to this work.

Funding statement:
- This research report was supported by grants from the National Natural Science Foundation of China (NSFC, No. 82130071 and 82072516), the National Key Innovation Team of China (No. 4174DH), and The Creative Research Groups Of Natural Science Foundation Of Chongqing (No. cstc2020jcyj-cxttX0004).

ICMJE COI statement:
- The authors declare that they have no conflicts of interest.

Data sharing:
- The data supporting the findings of this study are available within the article and its supplementary information files.

Acknowledgements:
- We appreciate the support from Chongqing Institute of Bio-intelligent Manufacturing, Chongqing, China.

Ethical review statement:
- All procedures performed in studies involving animals were in accordance with the ethical standards of the institution at which the studies were conducted, and ethical approval was obtained from the Ethics Committee and the Institutional Animal Care, Southwest Hospital and Army Medical University Consent to participate.

Open access funding:
- The authors report that they received open access funding for their manuscript from the National Natural Science Foundation of China (NSFC, No. 82130071).